Arch Microbiol (2009) 191:441–450
DOI 10.1007/s00203-009-0471-1

ORIGINAL PAPER

# Localization and characterization of VVA0331, a 489-kDa RTX-like protein, in *Vibrio vulnificus* YJ016

**Li-Fang Chou · Hwei-Ling Peng · Yu-Chung Yang · Min-Chieh Kuo · Hwan-You Chang**

Received: 18 December 2008 / Revised: 19 February 2009 / Accepted: 6 March 2009 / Published online: 27 March 2009


**Abstract** *Vibrio vulnificus* YJ016 contains three genes encoding proteins homologous to repeats-in-toxin proteins. One of these genes, *vva0331*, possesses a long open reading frame of 13,971 bp in length and resides on the small chromosome between two gene clusters encoding a type I secretion system and several regulatory proteins, respectively. Bioinformatic analysis revealed that VVA0331 consist of nineteen 87-amino acid repeats, two Arg-Gly-Asp motifs, four cysteine residues, an outer membrane protein domain, a polysaccharide-binding site and several motifs related to cell adhesions. These features are distinct from those of typical repeat-in-toxins and autotransporter adhesins. Real-time quantitative PCR analysis indicates that *vva0331* gene expression is activated at 30°C and regulated by iron. In addition, VVA0331 is present primarily in a secreted form as determined by cell fractionation assay and Western blot analysis. No significant difference in Hep2 cell adherence, cytotoxicity, and virulence was observed between the wild type and *vva0331* mutant strains. In contrast, these strains exhibited apparently different outer membrane protein profiles, and antiserum raised against C-terminal region of VVA0331 reacted with an 85-kDa outer membrane protein of *V. vulnificus* YJ016.

**Keywords** *Vibrio vulnificus* · RTX · Agglutination · Outer membrane proteins

**Abbreviations**

| | |
|---|---|
| RTX | Repeats-in-toxin |
| TISS | Type I secretion system |
| VcRtxA | *Vibrio cholerae* RtxA |
| Q-PCR | Real-time quantitative PCR |
| g3pdh | Glyceraldehyde-3-phosphate dehydrogenase |
| OmpA | Outer membrane protein A |
| TCA | Trichloroacetic acid |
| CHO | Chinese hamster ovary cells |
| vWf | Von Willebrand factor |

## Introduction

*Vibrio vulnificus*, a motile Gram-negative rod-shaped bacterium, is a natural habitant of marine environments. The microorganism causes three major syndromes in human hosts: wound infection, primary septicemia, and gastroenteritis. The mortality rate in soft patients with tissue infection caused by the pathogen is about 25%, in septic patients is up to 50%, and for all three illnesses is 37% (Blake et al. 1979; Chiang and Chuang 2003; Gulig et al. 2005). Additionally, *V. vulnificus* infections frequently occurred in individuals with liver diseases or immunosuppression.

*Vibrio vulnificus* can express various virulence-associated factors, including capsular polysaccharides, lipopolysaccharides, extracellular hemolysin/cytolysin, metalloprotease, pili,

Communicated by Jorge Membrillo-Hernández.

**Electronic supplementary material** The online version of this article (doi:10.1007/s00203-009-0471-1) contains supplementary material, which is available to authorized users.

L.-F. Chou · M.-C. Kuo · H.-Y. Chang (✉)
Institute of Molecular Medicine,
National Tsing Hua University, Hsin Chu, Taiwan, ROC
e-mail: hychang@life.nthu.edu.tw

L.-F. Chou
e-mail: d928209@oz.nthu.edu.tw

H.-L. Peng · Y.-C. Yang
Department of Biological Science and Technology,
National Chiao Tung University, 300 Hsin Chu, Taiwan, ROC

flagella, siderophore, and repeats-in-toxin (RTX) proteins (Chiang and Chuang 2003; Gulig et al. 2005). The RTX proteins are commonly secreted by a type I secretion system (TISS) and are present widely in Gram-negative human and animal pathogens. The common structure of RTX includes a carboxyl-terminal calcium-binding domain of acidic glycine-rich nonapeptide repeats. A typical *rtx* operon comprises four genes, *rtxA, rtxC, rtxB*, and *rtxD,* encoding the cytolytic toxin, an essential acyltransferase, an ATP-binding cassette transporter, and an uncharacterized protein, respectively (Coote 1992; Lally et al. 1999). The *Vibrio cholerae* RtxA (VcRtxA) has cytotoxic activity and cell rounding ability resulting from depolymerization of actin cytoskeleton (Lin et al. 1999; Fullner and Mekalanos 2000; Sheahan et al. 2004). Recent findings further suggest that VcRtxA is associated with growth phase regulation and is independent of quorum sensing (Boardman et al. 2007).

The genomic DNA sequence of *V. vulnificus* YJ016, a strain isolated from a primary septicemia patient, has been determined (GenBank accession number NC_005140) (Chen et al. 2003). Three *rtx* loci were annotated in the genome: a complete *rtx* gene cluster (*vva1030-6*) and an incomplete set (*vva0331-3*) lacking *rtxC* are on the smaller chromosome; another *rtxA* gene *vv1546* is on the large chromosome. The gene *vva1030* (GenBank accession number NP_937086) encodes a product essential for cytotoxicity in INT-407 cells and virulence in mice (Lee et al. 2007), whereas the functions of the other two *rtxA* genes, *vva0331* (NP_936387) and *vv1546* (NP_934339), remain obscure.

This study attempts to identify the functional role of *vva0331*, which encodes a protein with a theoretical mass of 489 kDa and a pI of 3.57. Here we report the effect of different growth condition on *vva0331* expression and the subcellular location of the gene product. Several biological properties of a *vva0331* knockout mutant were also characterized. The findings provide important implication on the possible functional roles of the large RTX-like protein.

## Materials and methods

### Bacterial strains and growth conditions

The bacterial strains used in this study are listed in Table S1. *V. vulnificus* YJ016 (Chen et al. 2003) and its derivatives were propagated at 30°C in Luria-Bertani (LB) broth supplemented with 100 U $ml^{-1}$ polymyxin B (Sigma-Aldrich Co., St. Louis, MO). For growth in iron-replete conditions, M9 minimal medium supplemented with either 10 μM ferric iron or 10 μM ferrous iron was used (Neilands 1981). Iron-limiting conditions were achieved by addition of the iron chelator 2, 2′—dipyridyl (Sigma-Aldrich Co.) to a final concentration of 100 μM in M9 medium (Mourino et al. 2004).

### Database and bioinformatic analysis

The sequences of *vva0331-5* were retrieved from the GenBank. The protein motif identification was analyzed by using Pfam, ScanProsite, RADAR and EMBL-EBI databases. Dot-matrix plots were produced by using the DOTMATCHER program in the EMBOSS database (http://www.emboss.sourceforge.net/apps/cvs/) at a threshold of 30. A line parallel to the diagonal line in the output dot-matrix plot indicates a direct repeat. The distance between two parallel lines indicates the smallest repeat units. A line exhibiting a higher dot density indicates a higher similarity between the repeats. Thus, a dark square in the plot represents multiple short tandem repeats.

### RNA purification and Q-PCR

Total RNA was purified from mid-log-phase cultures of *V. vulnificus* YJ016 grown in LB broth under different environmental stimuli by using the TRI reagent. First-strand cDNA was synthesized from 2 μg of DNase-treated RNA samples in a 20 μl reaction volume using the SuperScript First-strand cDNA Synthesis System (Life Technologies, Carlsbad, CA). The real-time quantitative PCR (Q-PCR) assays were performed by using ABI PRISM® 7500 Sequence Detection System and a SYBR-Green PCR kit (Life Technologies). The threshold cycle ($C_T$) values were used to determine relative RNA levels of glyceraldehyde-3-phosphate dehydrogenase (*g3pdh*) and *vva0331* genes. Primers specific to *vva0331* (forward, 5′-CCGGAATTCA CTTGGTACTTTGATCAT-3′; reverse, 5′-TCTGCCAGT GGTTGACGACTTAGT-3′) and *g3pdh* (forward, 5′-TGA CTATCAAAGTGGGAATTAACGG-3′; reverse, 5′-ATC GAACTCCGATAGGTGCCCAAT-3′) were used to amplify fragments about 200 bp in length. Statistical analysis was performed using a Student's *t* test (SigmaPlot version 9; Systat Software Inc.) from biologically duplicate samples. Difference was considered significant if *P* values were <0.01. Data with *P* values <0.001 are indicated by two asterisks, whereas data with *P* values between 0.001 and 0.01 are indicated by a single asterisk.

### Generation of *vva0331* knockout mutants

For localization and functional studies of the *vva0331* gene product, two *vva0331* mutant strains with a deletion at two distinct regions of the gene were generated via the allelic exchange strategy. Strain EY331 suffers an 800-bp out-of-frame deletion (nucleotide positions 1,917 to 2,737) at the repeat containing region. The other strain, LF138, has a

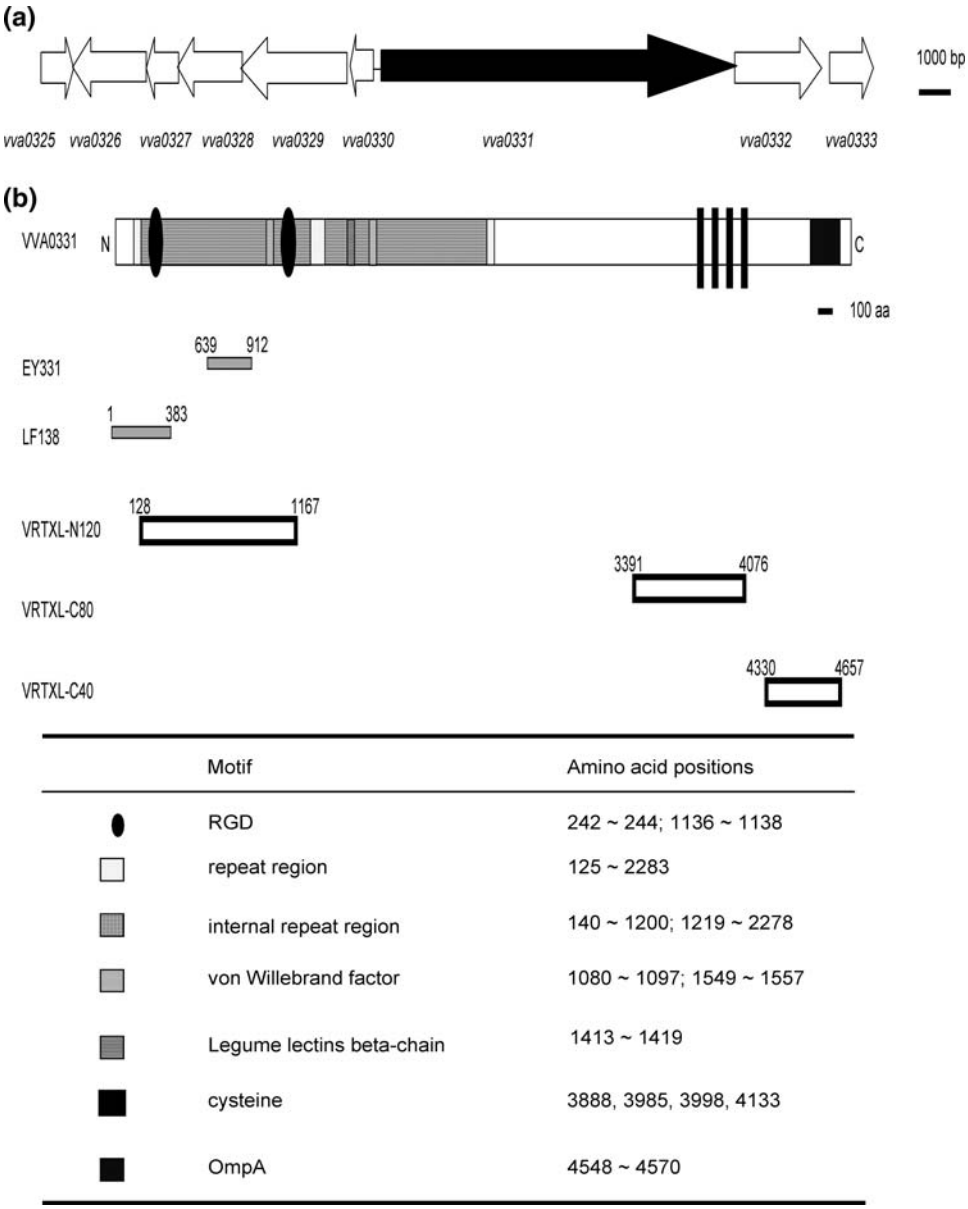


**Fig. 1** Schematic representation of *vva0331* gene cluster and motif organization of the gene product. **a** Organization of the *vva0331* gene cluster. The figure was constructed based on the nucleotide sequence of *V. vulnificus* YJ016 (accession no. NC_005140). The *arrows* indicate the transcription direction and the gene IDs are shown below each coding region. The predicted functions are as follows: response regulator (*vva0325*), GGDEF family protein (*vva0326*), response regulator (*vva0327*), putative two-component response regulator with EAL domain (*vva0328*), sensor kinase VieS (*vva0329*), putative RTX toxin (*vva0331*; black shading), RtxB-like secretion ATP-binding protein (*vva0332*), and RtxD-like transport protein (*vva0333*). **b** VVA0331 motif organization. Regions deleted in *vva0331* mutants (EY331 and LF138) and truncated VVA0331 recombinant fragments (VRTX-N120, VRTX-C80 and VRTX-C40) for antisera preparation are shown

1.1 kb deletion (nucleotide positions 1–1,149) comprising the translation initiation codon and the first RGD site (Fig. 1b). The deletions in these mutant strains were confirmed by PCR, nucleotide sequencing, and Southern blot analyses (Fig. S1).

## Heterologous expression of truncated VVA0331 proteins and preparation of their specific antibodies

Three hexa-His tagged fusion proteins: LF-N120 containing residues 128-1167 (VRTXL-N120), LF-C80 containing residues 3391-4076 (VRTXL-C80), and LF-C40 containing residues 4330-4657 (VRTXL-C40), were, respectively, produced in *Escherichia coli*, purified by using a nickel-affinity chromatography column, and used in antibody generation in BALB/c mice (Fig. 1b). Mice were injected intraperitoneally at 2-week intervals with the purified protein in complete Freund's adjuvant (Sigma Chemical Co.), then a booster injection of the purified protein emulsified with incomplete Freund's adjuvant (Sigma Chemical Co.), and finally one further booster with the antigen alone. Blood samples were collected from the tail of the immunized mice, allowed to clot at room temperature, and sera were stored at −20°C.

## Subcellular localization of VVA0331 in *V. vulnificus* YJ016

To determine the location of the 489-kDa RTX-like protein in *V. vulnificus* YJ016, a fractionation assay of bacterial components was performed as previously described (Boardman and Satchell 2004; Boardman et al. 2007). Concen-

trated culture supernatants were prepared from 100-ml bacterial cultures grown to an optical density of 0.4–0.6 at 600 nm at 30°C. Bacteria were precipitated by centrifugation, and the supernatant was filtered through a 0.45-μm pore size Acrodisc® syringe filter (Pall) to remove residual bacterial cells. An equal volume of 20% trichloroacetic acid (TCA) was added to the supernatant to precipitate secreted proteins. For preparation of cell membrane and cytoplasmic fractions, the bacterial pellet was washed with 2 mM $CaCl_2$, resuspended in 1 ml of ice-cold distilled water, broken by sonication, and centrifuged at 100,000×*g* for 30 min. The clarified supernatant was collected and used as the cytoplasmic fraction. The pellet, representing the membrane fraction, was resuspended in 10 mM Tris–HCl (pH 8.0). Sodium lauroyl sarcosinate (Sarkosyl) extraction method was used to prepare outer membrane fraction as previously described elsewhere (Koga and Kawata 1986). The membrane fraction was treated with 0.5% Sarkosyl in 10 mM Tris–HCl buffer (pH 8.0) at 30°C for 30 min to solubilize inner membranes. The insoluble material was recovered by centrifugation at 200,000×*g* for 60 min, washed with and resuspended in distilled water, and used as the outer membrane preparation. The protein concentration was quantified by the Bradford protein assay (Bradford 1976) and these samples were resolved by using SDS-PAGE, transferred to PVDF membranes, and incubated sequentially with an anti-VVA0331 polyclonal antibody and a peroxidase-conjugated anti-mouse antibody. The VVA0331 proteins were detected by using a substrate kit (VECTOR$^R$ NovaRED™, Vector Laboratories, Inc.). The purity of these fractions was also confirmed by immunostaining with a rabbit polyclonal β-galactosidase antibody (ABcam # ab616). Protein size markers were the HiMark™ Prestained HMW protein standards (Invitrogen).

### Slide agglutination test

*Vibrio vulnificus* YJ016 agglutination was performed on glass slides by mixing 5 μl of the antiserum against VVA0331 with a loopful of bacterial suspension for 5 min, and examined under a light microscope. A distinct and immediately occurring agglutination was registered as positive, while weak or no agglutination in 5 min was considered negative.

### Immunofluorescence staining

To investigate whether VVA0331 is located on cell surface, an immunofluorescence staining was performed. Overnight grown bacteria were collected by centrifugation at 3,400×*g* for 5 min, and the precipitated cells were resuspended in 500 μl PBS containing 5% BSA, gently rocked for 1 h, and then incubated for 1 h with 500 μl of an anti-VVA0331 antibody at a dilution of 1:200 in PBS-5% BSA. After washing twice with 500 μl PBS, the bacterial cells were incubated for 1 h with 500 μl FITC-conjugated goat anti-mouse IgG at a 1: 100 dilution in PBS containing 5% BSA. The cells were washed three times with PBS, and resuspended in 50 μl PBS. One drop of the cell suspension was deposited onto a microscope slide, and viewed under an epifluorescence microscope.

### Cell adherence and cytotoxicity assays

Bacterial adherence assays (Lee et al. 2004) were performed on human laryngeal epithelial cell (HEp-2) monolayers grown in 24-well tissue culture plates in which approximately $10^5$ cells were seeded in each well and grown overnight at 37°C in 5% $CO_2$. The HEp-2 cell monolayers were washed twice with PBS, followed by the addition of serum-free MEM with Earle's salts, then inoculated with 100 μl of the diluted bacteria to give a multiplicity of infection of 10, and incubated for 1 h. The monolayers were then washed six times with PBS to remove non-adherent bacteria. Following the last wash, the cells were lysed with 0.1% Triton X-100 for 15 min. The bacteria were recovered from the cells, serially 10-fold diluted, plated on LB agar, and colony enumerated.

Cytotoxicity experiments were carried out on Chinese hamster ovary (CHO) cells seeded in 96-well tissue culture plates (Nunc, Denmark) at a density of $2 \times 10^4$ cells/well 24 h prior to the experiment (Paranjpye et al. 1998). Bacterial culture supernatant was centrifuged twice at 12,000×*g* and filtered through a 0.45-μm-pore-size Acrodisc® syringe filter to remove bacteria. Twenty microliters of the clarified culture supernatant was added to the CHO cell monolayer covered with 180 μl of serum-free F-12 medium and then incubated at 37°C in 5% $CO_2$ for 4 h. The cytotoxic activity was determined by measuring lactate dehydrogenase released from the cells using a Cytotox 96 Non-radioactive cytotoxic assay kit (Promega, Madison, WI).

### Mouse virulence assay

Pathogen-free female BALB/c mice of 6–8 weeks old were purchased from the Animal Center of National Taiwan University College of Medicine for preparation of antibodies and virulence assay. Studies with animals were performed with the approval of the Animal Ethics Committee of National Tsing Hua University. Groups of ($n = 6$) mice were challenged by intraperitoneal injection with 0.1 ml serial dilutions of the bacterial suspension in phosphate-buffered saline and mortality was recorded at 72 h post infection. The doses lethal to 50% of the mice ($LD_{50}$) were calculated by the method of Reed and Muench (1938).

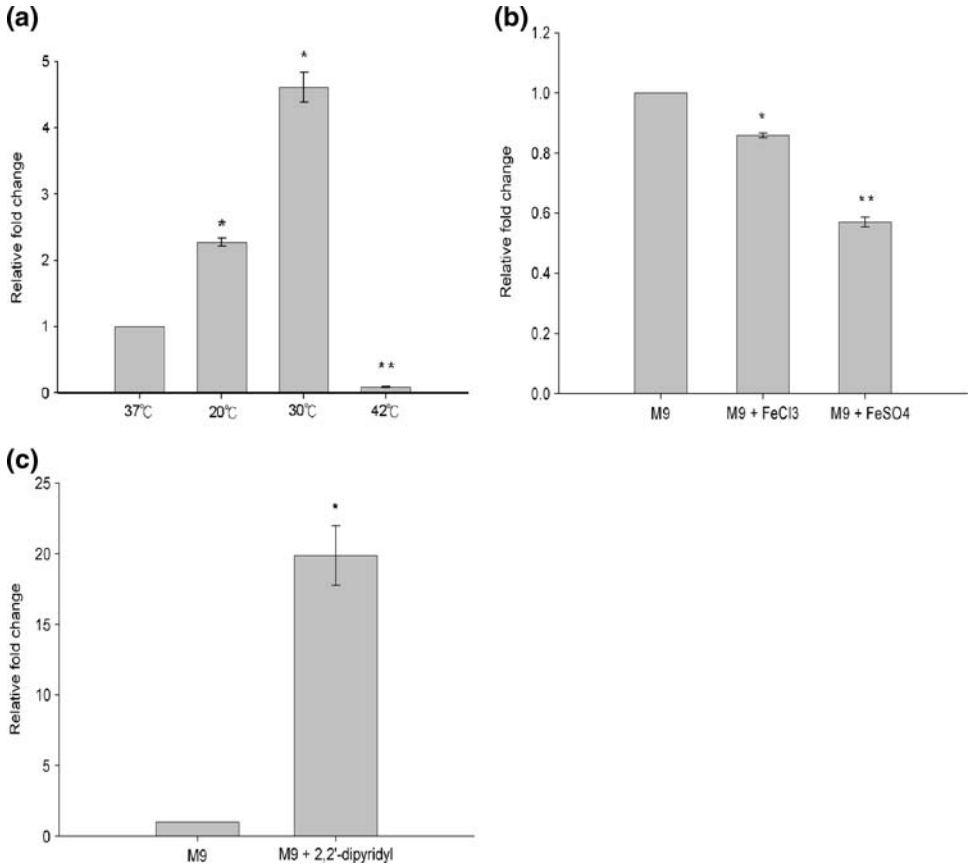


**Fig. 2** Expression of *vva0331*. The effects of different temperatures (**a**), 10 μM iron supplement (**b**), and iron-limiting conditions (**c**) on *vva0331* transcription were determined by Q-PCR. The data are the means ± standard deviations ($n = 2$). *Asterisks* indicate values statistically significantly different from the control values

## Results

### Organization of *vva0325-33* and functional domains in VVA0331

The *vva0331* belongs to a large gene cluster comprising genes encoding a partial TISS (*vva0332–vva0333*) and a VieSAB-like three-component signal transduction system (*vva0325–vva0329*) (Fig. 1a). VVA0331 is a very large protein which shares 27% sequence identity with a putative RTX family exoprotein in *E. coli* O157:H7 (Bauer and Welch 1996). It was also annotated as an autotransporter adhesin (*vv2_1514*) in *V. vulnificus* CMCP6. Previous repeat analysis using the RADAR program showed that the N-terminal half of VVA0331 is organized by 19 tandem repeats (Kuo et al. 2008). Use of the SMART program (Letunic et al. 2006; Kuo et al. 2008) also identified two internal repeats in the region (residues 140–1,200 and residues 1,219–2,278, respectively). In addition, it was noted that two RGD containing motifs and a Legume lectin domain in the N-terminal region, and an OMPA domain in the C-terminal region (Fig. 1b). The OmpA domain is a 22-residue signature present in C-terminal region of outer membrane proteins in many Gram-negative organisms. The domain is also required for interaction of *E. coli* with host molecules (De Mot et al. 1994; Hardham and Stamm 1994). Furthermore, a domain similar to von Willebrand factor (vWf), a large multimeric glycoprotein found in blood plasma, was predicted in VVA0331. Neither an N-terminal signal peptide nor trans-membrane helices were identified in VVA0331.

### Expression of *vva0331* in different growth conditions

Shifting from room temperature to 37°C upon entering a mammalian host is an important signal sensed by bacteria. We determined the effects of different temperatures on *vva0331* gene expression by using Q-PCR. The result demonstrated higher *vva0331* gene expressions at 30 and 20°C, increasing about 4.7-fold and 2.3-fold, respectively, compared to that at 37°C (Fig. 2a). The result suggests that *vva0331* is not critical for the bacterial infections. Iron, which plays a pivotal role in the pathogenesis of *V. vulnificus* infection and growth (Gulig et al. 2005), also affects *vva0331* gene expression. In the presence of 10 μM $Fe^{2+}$, *vva0331* gene expression reduced to half of the control (Fig. 2b). In contrast, a significant increase ($P < 0.01$) in *vva0331* gene expression was observed under iron-limiting conditions (Fig. 2c). Whether VVA0331 indeed participates in iron acquisition remains to be investigated.

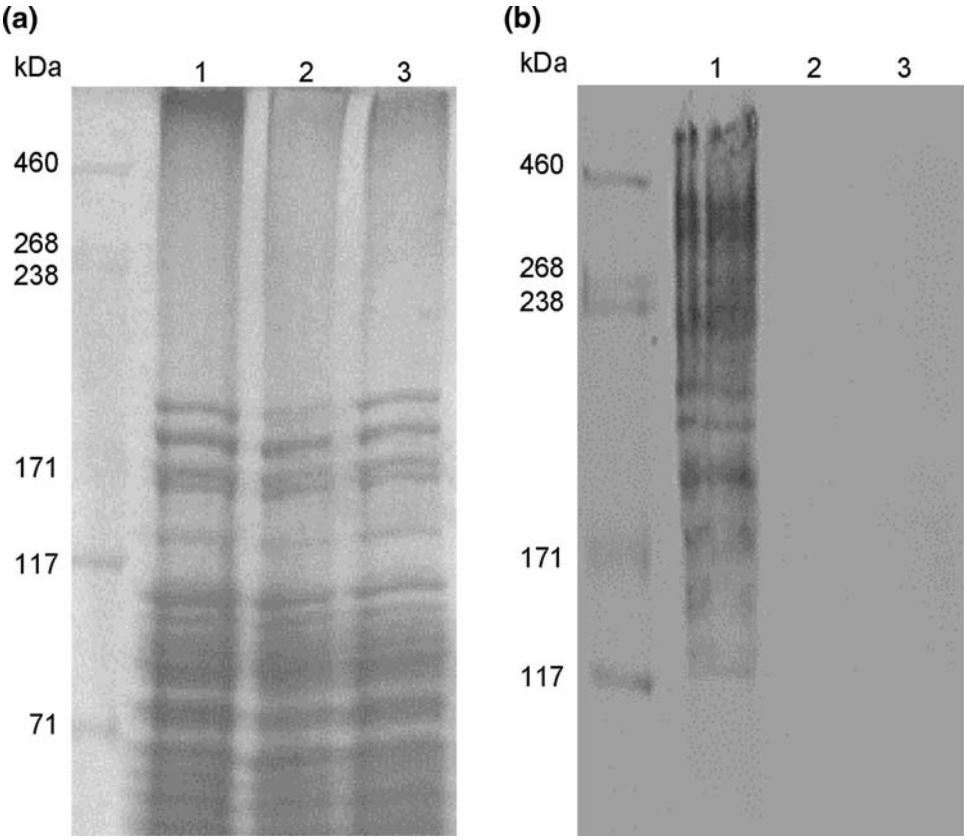


**Fig. 3** Detection of VVA0331 by Western blot analysis. Total cellular lysates of *V. vulnificus* YJ016 and the *vva0331* mutant strains grown in LB to stationary phase ($OD_{600}$ = 2.0) were examined for the presence of VVA0331 by electrophores is on 0.1% SDS-6% polyacrylamide gel, stained with Coomassie Blue (**a**), or immunostained using a mouse antiserum against VRTX-C80 (**b**). Lanes *1*, *V. vulnificus* YJ016; *2*, EY331; *3*, LF138. Molecular weight markers are shown on the left (in kDa)

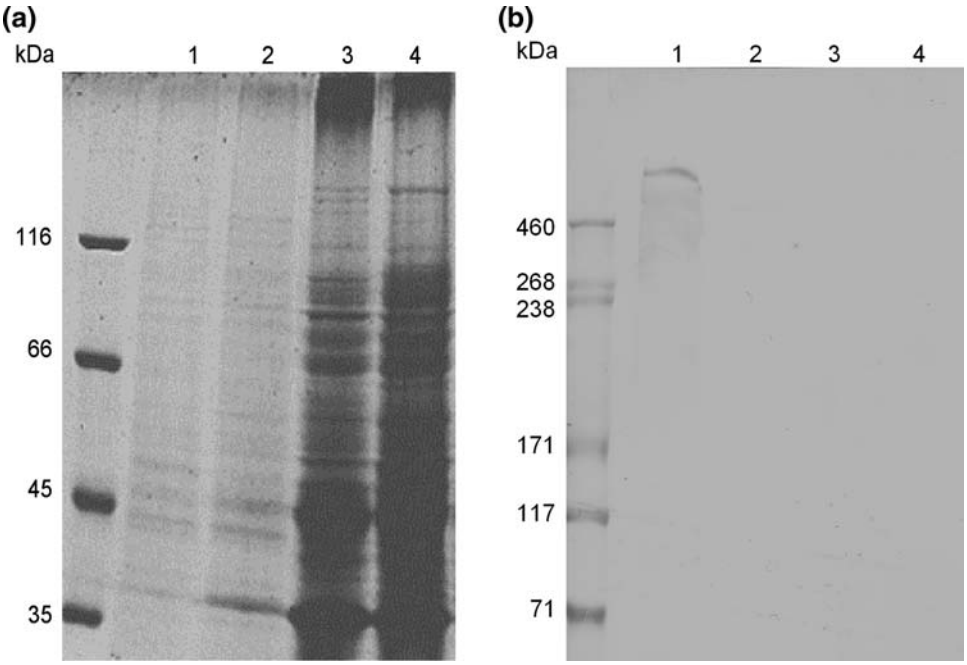


**Fig. 4** Localization of VVA0331 in different cellular fractions. TCA concentrated culture supernatant and membrane fractions were resolved on a 0.1% SDS-10% polyacrylamide gel and stained with Coomassie Brilliant Blue R250 (**a**), or on a 0.1% SDS-6% polyacrylamide gel and detected with an antiserum specific to VRTXL-C80 (**b**). Lanes *1* and *2*, TCA concentrated culture supernatant; *3* and *4*, membrane fraction. Lanes *1* and *3*, *V. vulnificus* YJ016; *2* and *4*, EY331. Molecular weight markers are shown on the left (in kDa)

Localization of the 489-kDa RTX-like protein, VVA0331, in *V. vulnificus* YJ016

Three recombinant hexaHis-tagged fusion proteins, VRTXL-N120, VRTXL-C80, and VRTXL-C40, covering different regions of VVA0331 were constructed and used to generate antibodies in laboratory mice. The antibodies generated with VRTXL-N120, VRTXL-C40, and VRTXL-C80 could recognize a protein of approximately 500 kDa in size specifically in the total cell lysates of wild type strain but not in the EY331 and LF138 strains, as confirmed by Western blot analysis (Fig. 3 and Fig. S2). The anti-VRTXL-C80 serum

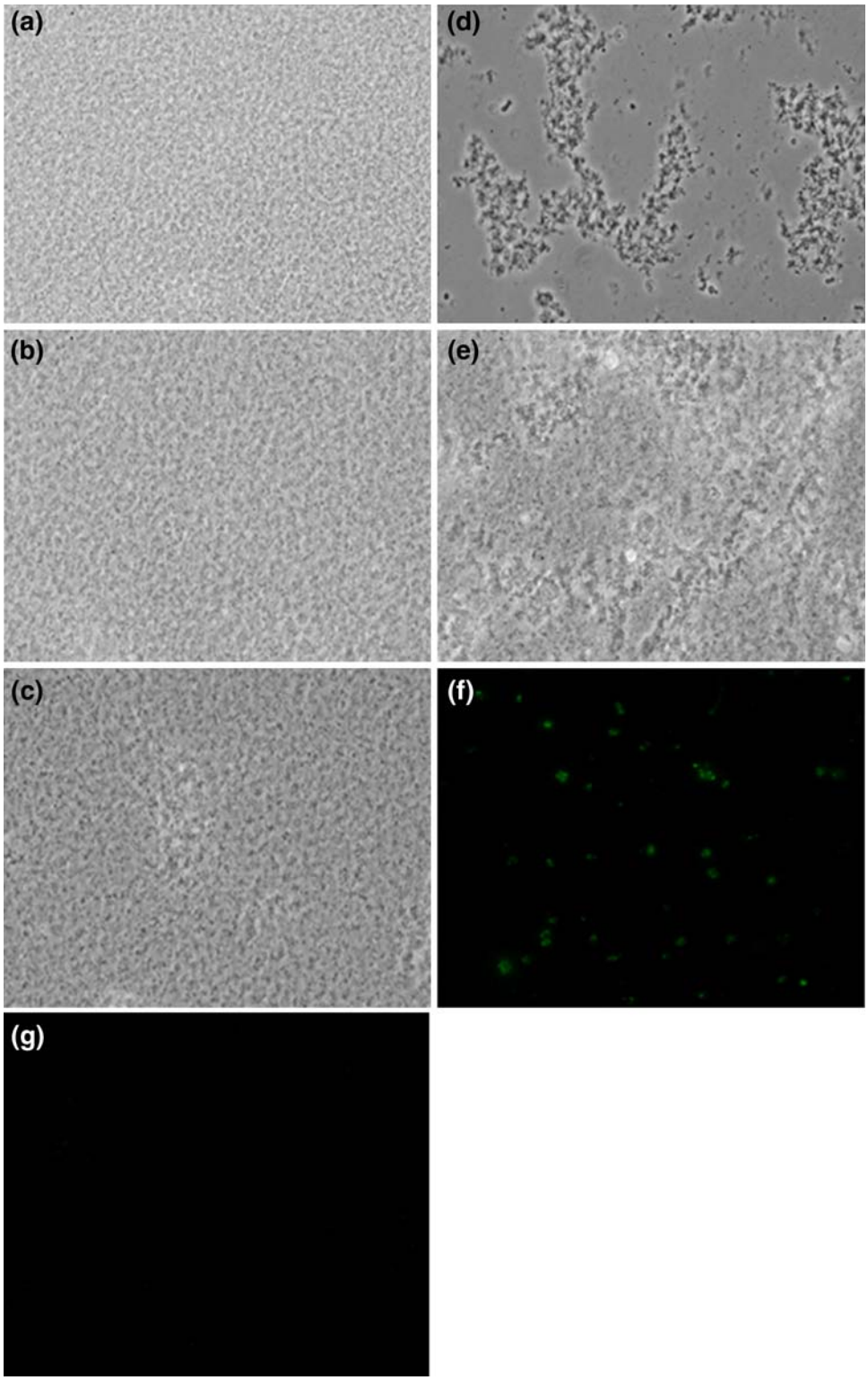


**Fig. 5** Agglutination of *V. vulnificus* with mouse antisera specific to different VVA0331 regions. The bacteria incubated with different antisera were examined directly under a light microscope (400X) (**a**–**e**) or a fluorescence microscope after immunofluorescent staining (1000X) (**f**–**g**). (**a**) YJ016/0.85% NaCl (**b**) YJ016/anti-VRTXL-N120 serum (**c**) YJ016/anti-VRTXL-C80 serum (**d**) YJ016/anti-VRTXL-C40 serum (**e**) EY331/anti-VRTXL-C40 serum (**f**) YJ016/anti-VRTXL-C40 serum (**g**) YJ016/anti-VRTXL-N120 serum

was selected for VVA0331 localization due to its lower background.

To determine the location of VVA0331 in *V. vulnificus* YJ016, different subcellular fractions were collected, respectively, from *V. vulnificus* YJ016 and EY331. The ~500-kDa protein band could be observed in culture supernatant, but not in the membrane fraction of *V. vulnificus* YJ016 (Fig. 4). The purity of the fractions was verified by using an antibody recognizing cytoplasmic protein β-galactosidase (Fig. S3). The protein band intensity was rather

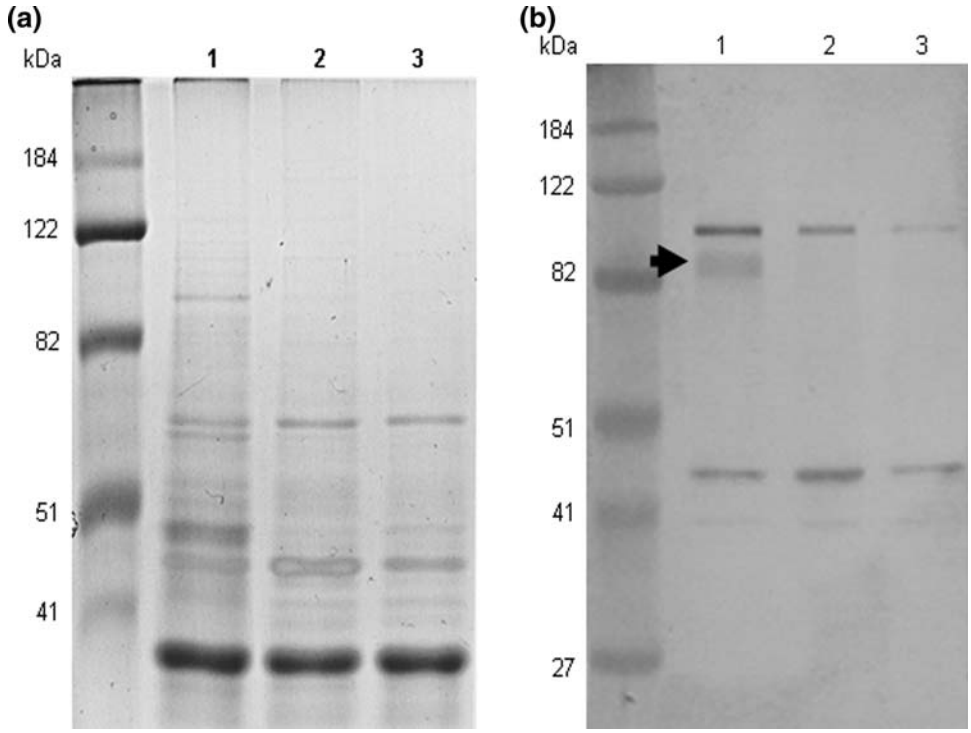


**Fig. 6** Outer membrane protein profiles of *V. vulnificus* YJ016 and *vva0331* deletion mutants. The proteins were resolved on a 0.1% SDS-10% polyacrylamide gel and visualized by staining with Coomassie Blue (**a**), or immunostaining with antiserum against VRTXL-C40 (**b**). Lanes *1*, *V. vulnificus* YJ016; *2*, EY331; *3*, LF138. The ~85 kDa protein is marked by an *arrowhead*. The sizes of the molecular weight markers (BMA ProSieve Color Protein Markers; Rockland, ME) are shown on the left (in kDa)

weak suggesting that VVA0331 is secreted by *V. vulnificus* YJ016 in low quantities.

### Agglutination of *V. vulnificus* YJ016 by anti-VRTXL-C40 serum

Unlike anti-VRTX-N120 and anti-VRTX-C80 sera, which recognize VVA0331 in both cell-bound fraction and culture supernatant, anti-VRTXL-C40 detected a ~500-kDa protein band in cell-bound but not in the culture supernatant fraction (Fig. S2). Evaluation of these sera by slide agglutination revealed that anti-VRTXL-C40 serum, but not the other two antisera, agglutinated *V. vulnificus* YJ016 efficiently (Fig. 5a–e). Furthermore, binding of polyclonal sera against VRTX-C40 to the cell surface of *V. vulnificus* YJ016 could be detected by immunofluorescence staining, indicating that the C-terminal region of VVA0331 is present in the outer membrane of *V. vulnificus* (Fig. 5f–g). In contrast, VRTX-N120 yielded only background immunofluoresence on *V. vulnificus* YJ016.

### The C-terminal portion of VVA0331 is located on the outer membrane

The presence of the C-terminal region of VVA0331 on the outer membrane of *V. vulnificus* was further confirmed by Western blot analysis. Anti-VRTXL-C40 serum specifically detected a major protein band of approximately 85 kDa only in *V. vulnificus* YJ016 as well as several nonspecific proteins in both *V. vulnificus* wild type and mutant strains (Fig. 6). The result suggests that the C-terminal region of VVA0331 was cleaved and present in the outer membrane of the bacterium.

### Effect of *vva0331* deletions on cell adherence, cytotoxicity, and mouse lethality of *V. vulnificus*

As the C-terminal portion of VVA0331 is located on the outer membrane, we speculate that the protein may play a role in the bacterial adhesion on the host cells. Nevertheless, standard bacterial adherence assay on the HEp-2 cells did not reveal a significant difference between *V. vulnificus* YJ016 and EY331, both retaining about 4–5% of input bacteria on the HEp-2 cell monolayer after extensive washing.

The cytotoxicity of the *vva0331* mutant strains to CHO cell line and their virulence in BALB/c mice were determined. The wild type and mutant strains were equally cytotoxic to CHO cells and exhibit a $LD_{50}$ of 1–3 × $10^6$ CFU (data not shown). These results showed no apparent difference between *V. vulnificus* YJ016 and EY331, indicating that VVA0331 does not play major roles in these events.

## Discussion

Unlike described previously (Chen et al. 2003), our bioinformatic analysis of VVA0331 sequence shows that the structural features of the protein are distinct from typical RTX proteins and autotransporter adhesins. For example, the N-terminal region contains a repeat region but lacks a

pore-forming domain and the repeats are different from the nine-residue glycine-rich repeats commonly found in the C-terminal region of RTX toxins. Recently, Satchell (Satchell 2007) renamed *V. cholerae* RtxA toxin as multifunctional autoprocessing RTX toxin, or MARTX, which represents a larger group of RTX toxins produced by at least eight Gram-negative species, including those in the genera *Vibrio*, *Aeromonas*, and *Yersinia*. The MARTX toxins are distinguished from other RTX toxins by both their large size (>400 kDa) and novel repeat structures. Nevertheless, comparison of the repeat sequences in VVA0331 and *V. vulnificus* RtxA, a MARTX protein, indicates that VVA0331 does not have the same novel A, B, and C repeat structures proposed for the MARTX toxins either in the repeat length, relative locations or sequence similarity (Fig. 7c), and thus likely represents a new family of RTX toxins.

A vWf domain and bacterial Ig-like domains were predicted in VVA0331. Proteins that incorporate the vWf domain participate in numerous biological events such as cell adhesion, migration, homing, pattern formation, and signal transduction (Colombatti et al. 1993). The bacterial Ig-like domain is commonly found in a variety of bacterial and phage surface proteins, implying a role in cell adhesion (Kelly et al. 1999). All these bioinformatic findings suggest that VVA0331 may be an adhesion protein. Nevertheless, we were unable to observe significant difference in HEp-2 cell adherence between the wild type and a *vva0331* mutant strain. However, this finding does not rule out the possibility that VVA0331 may contribute to *V. vulnificus* binding to other cell types or non-cellular surfaces.

It is not clear how VVA0331 is secreted because the N-terminus of VVA0331 does not possess a secretion signal sequence. No significant consensus secretion features in related proteins such as hemolysin (Kenny et al. 1992; Lin et al. 1999) and autotransporters could be observed in VVA0331. Furthermore, the TISS encoding gene cluster adjacent to *vva0331* is incomplete and lacks *rtxC* which aids in the maturation of exported RTX proteins (Henderson and Nataro 2001; Desvaux et al. 2004). These findings suggest that VVA0331 employs a novel secretion mechanism. Interestingly, this study also shows that the C-terminal region of VVA0331 is retained on *V. vulnificus* YJ016 outer membrane. Consistent with the finding, bioinformatic analysis has identified a possible outer membrane protein domain in the VVA0331 C-terminal region.

The Q-PCR analysis demonstrated an up-regulation of *vva0331* at iron-limiting condition indicating that the gene is regulated by iron. However, we did not find the Fur box or a transcription factor binding site related to iron regulation within the upstream control region of *vva0331* by regulon prediction and promoter analysis of Virtual Footprint (Munch et al. 2005) and the program BPROM (SoftBerry, Mount Kisco, NY).

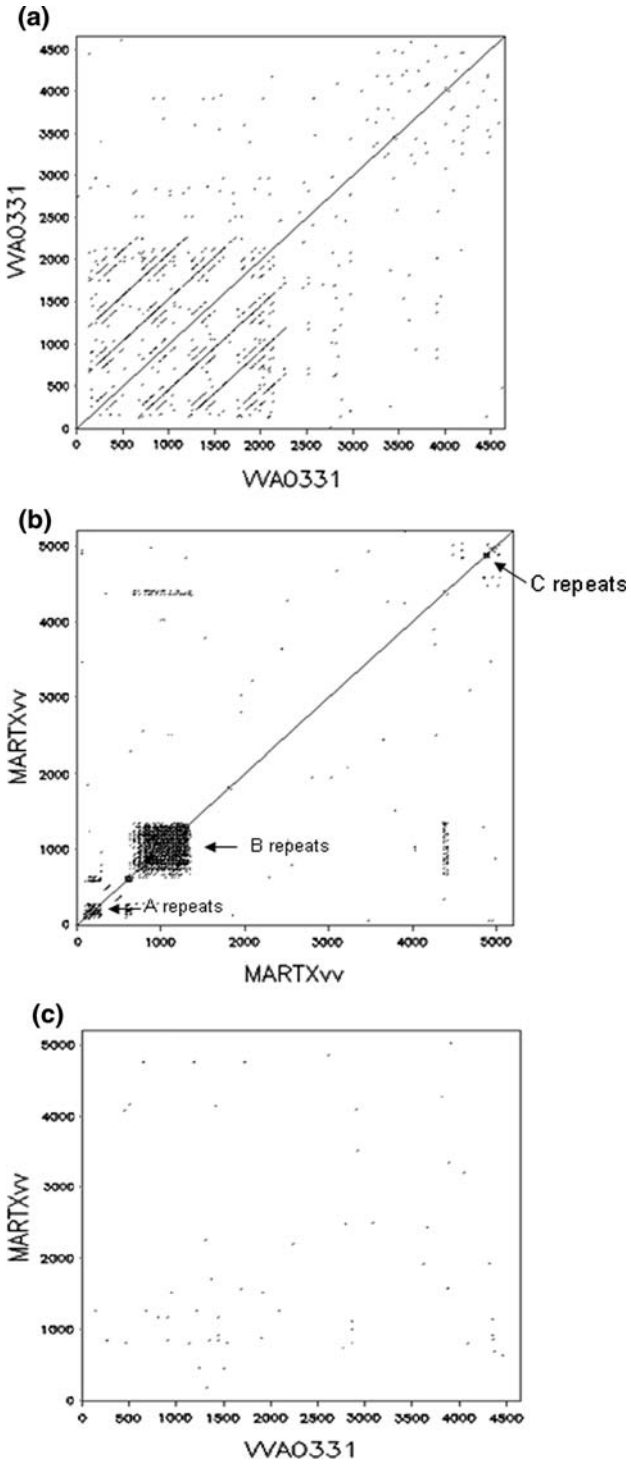


**Fig. 7** Comparison of repeat regions in VVA0331 and *V. vulnificus* RtxA (MARTX toxin, GenBank Accession Number NP_937086.1). Dot-matrix plots were produced by using the DOTMATCHER program at a threshold of 30. (**a**) VVA0331 vs. VVA0331; (**b**) *V. vulnificus* RtxA; (**c**) VVA0331 vs. *V. vulnificus* RtxA. The locations of A, B, and C repeats proposed for MARTX proteins are indicated in (**b**)

Our results demonstrate that VVA0331 protein was secreted from *V. vulnificus* YJ016 in exponential growth phase. Nevertheless, the functional roles of VVA0331

remain elusive. It may be worth pointing out that Rhee et al. have not only examined the deletion mutant of *vv2_1514*, an orthologous locus of *vva0331* in *V. vulnificus* CMCP6, but also failed to detect significant decreases in the bacterial cytotoxicity (Kim et al. 2008). Thus, VVA0331 may play only a minor role in bacterial virulence. A *vva0331* and *vva1030* double mutant may provide better answers in this aspect.

In conclusion, we describe the expression and localization of a very large RTX-like protein in *V. vulnificus*. Mutants with a deletion at this locus showed very little discernible biological properties. Nevertheless, bioinformatic prediction and its localization properties all suggest that *vva0331* likely plays a role to aid *V. vulnificus* adhere and survive in the environments.

**Acknowledgments** This study was supported in part by the National Science Council of R.O.C. and NTHU-CGMU collaboration Fund. We thank Professor Lien-I Hor, Department of Microbiology and Immunology, National Cheng-Kung University, for generously providing *V. vulnificus* YJ016.

## References

Bauer ME, Welch RA (1996) Characterization of an RTX toxin from enterohemorrhagic *Escherichia coli* O157:H7. Infect Immun 64:167–175

Blake PA, Merson MH, Weaver RE, Hollis DG, Heublein PC (1979) Disease caused by a marine Vibrio: clinical characteristics and epidemiology. N Engl J Med 300:1–5

Boardman BK, Satchell KJ (2004) *Vibrio cholerae* strains with mutations in an atypical type I secretion system accumulate RTX toxin intracellularly. J Bacteriol 186:8137–8143

Boardman BK, Meehan BM, Fullner Satchell KJ (2007) Growth phase regulation of *Vibrio cholerae* RTX toxin export. J Bacteriol 189:1827–1835

Bradford MM (1976) A rapid and sensitive method for the quantitation of microgram quantities of protein utilizing the principle of protein-dye binding. Anal Biochem 72:248–254

Chen CY et al (2003) Comparative genome analysis of *Vibrio vulnificus*, a marine pathogen. Genome Res 13:2577–2587

Chiang SR, Chuang YC (2003) *Vibrio vulnificus* infection: clinical manifestations, pathogenesis, and antimicrobial therapy. J Microbiol Immunol Infect 36:81–88

Colombatti A, Bonaldo P, Doliana R (1993) Type A modules: interacting domains found in several non-fibrillar collagens and in other extracellular matrix proteins. Matrix 13:297–306

Coote JG (1992) Structural and functional relationships among the RTX toxin determinants of gram-negative bacteria. FEMS Microbiol Rev 8:137–161

De Mot R et al (1994) Molecular characterization of the major outer-membrane protein OprF from plant root-colonizing Pseudomonas fluorescens. Microbiology 140(Pt 6):1377–1387

Desvaux M, Parham NJ, Henderson IR (2004) The autotransporter secretion system. Res Microbiol 155:53–60

Donnenberg MS, Kaper JB (1991) Construction of an eae deletion mutant of enteropathogenic *Escherichia coli* by using a positive-selection suicide vector. Infect Immun 59:4310–4317

Fullner KJ, Mekalanos JJ (2000) In vivo covalent cross-linking of cellular actin by the *Vibrio cholerae* RTX toxin. EMBO J 19:5315–5323

Gulig PA, Bourdage KL, Starks AM (2005) Molecular pathogenesis of *Vibrio vulnificus*. J Microbiol 43 Spec No: 118–131

Hardham JM, Stamm LV (1994) Identification and characterization of the Treponema pallidum tpn50 gene, an ompA homolog. Infect Immun 62:1015–1025

Henderson IR, Nataro JP (2001) Virulence functions of autotransporter proteins. Infect Immun 69:1231–1243

Kelly G et al (1999) Structure of the cell-adhesion fragment of intimin from enteropathogenic *Escherichia coli*. Nat Struct Biol 6:313–318

Kenny B, Taylor S, Holland IB (1992) Identification of individual amino acids required for secretion within the haemolysin (HlyA) C-terminal targeting region. Mol Microbiol 6:1477–1489

Kim YR et al (2008) *Vibrio vulnificus* RTX toxin kills host cells only after contact of the bacteria with host cells. Cell Microbiol 10:848–862

Koga T, Kawata T (1986) Composition of major outer membrane proteins of *Vibrio vulnificus* isolates: effect of different growth media and iron deficiency. Microbiol Immunol 30:193–201

Kuo MC, Chou LF, Chang HY (2008) Evolution of exceptionally large genes in prokaryotes. J Mol Evol 66:333–349

Lally ET, Hill RB, Kieba IR, Korostoff J (1999) The interaction between RTX toxins and target cells. Trends Microbiol 7:356–361

Lee JH et al (2004) Role of flagellum and motility in pathogenesis of *Vibrio vulnificus*. Infect Immun 72:4905–4910

Lee JH et al (2007) Identification and characterization of the *Vibrio vulnificus* rtxA essential for cytotoxicity in vitro and virulence in mice. J Microbiol 45:146–152

Letunic I, Copley RR, Pils B, Pinkert S, Schultz J, Bork P (2006) SMART 5: domains in the context of genomes and networks. Nucleic Acids Res 34:D257–D260

Lin W et al (1999) Identification of a *vibrio cholerae* RTX toxin gene cluster that is tightly linked to the cholera toxin prophage. Proc Natl Acad Sci USA 96:1071–1076

Mourino S, Osorio CR, Lemos ML (2004) Characterization of heme uptake cluster genes in the fish pathogen *Vibrio anguillarum*. J Bacteriol 186:6159–6167

Munch R et al (2005) Virtual Footprint and PRODORIC: an integrative framework for regulon prediction in prokaryotes. Bioinformatics 21:4187–4189

Neilands JB (1981) Iron absorption and transport in microorganisms. Annu Rev Nutr 1:27–46

Paranjpye RN, Lara JC, Pepe JC, Pepe CM, Strom MS (1998) The type IV leader peptidase/N-methyltransferase of Vibrio vulnificus controls factors required for adherence to HEp-2 cells and virulence in iron-overloaded mice. Infect Immun 66:5659–5668

Reed H, Muench LJ (1938) A simple method of estimating the 50% endpoints. Am J Hyg 27:493–497

Satchell KJ (2007) MARTX, multifunctional autoprocessing repeats-in-toxin toxins. Infect Immun 75:5079–5084

Sheahan KL, Cordero CL, Satchell KJ (2004) Identification of a domain within the multifunctional *Vibrio cholerae* RTX toxin that covalently cross-links actin. Proc Natl Acad Sci USA 101:9798–9803